Self-Buckling of Micromachined Beams Under Resistive Heating

Mu Chiao and Liwei Lin, *Member, IEEE*

***Abstract*—Self-buckling behavior of micromachined beams under resistive heating is described by an electromechanical model with experimental verifications. This model consists of both electro-thermal and thermo-elastic analyses for beam-shape polysilicon microstructures that are fabricated by a standard surface micromachining process. When an input electrical current is applied, joule-heating effects trigger the thermal expansion of beam structures and cause mechanical buckling. The standard testing devices are clamped–clamped bridges, 2-μm wide, 2-μm thick, and 100-μm long. It is found that a minimum current of 3.5 mA is required to cause beam buckling. Under an input current of 4.8 mA, a lateral deflection of 2.9$\pm$0.2 μm at the center of the bridge is measured with a computer image processing scheme. The experimental measurements are found to be consistent with analytical predictions. A discussion of modeling considerations and process variations is presented. [412]**

***Index Terms*—Electro-thermal response, micro beams, post-buckling, resistive heating, thermal actuators, thermal buckling, thermoelasticity.**

Nomenclature

- A Cross-sectional area.
- E Young's modulus.
- F Thermal conductive shape factor.
- I Moment of inertia.
- J Current density.
- k Thermal conductivity.
- L Original length of the micro beam.
- P Thermal load.
- T Variable in the temperature equation.
- h Thickness.
- lift Suspension distance.
- s Coordinate along the actuated beam.
- x Coordinate along the horizontal axis.
- y Lateral deflection.
- α Thermal expansion coefficient.
- β Variable in substitution for $\theta_{\max}$.
- ρ Resistivity of polysilicon.
- ϵ Combined variable in heat equation.
- ε Strain.
- θ Deflection angle.
- ξ Thermal resistivity coefficient.
- ϕ Variable in substitution for $\theta_{\max}$ and β.

Subscript

- air Air.
- avg Average.
- com Combined variable.
- $\max$ Maximum.
- n Nitride.
- p Polysilicon.
- ∞ Ambient (bulk).

Manuscript received January 7, 1999; revised October 8, 1999. This work was supported in part by the National Science Foundation under CAREER Award ECS-9734421. Subject Editor, G. B. Hocker.

The authors are with the Department of Mechanical Engineering, The University of California at Berkeley, Berkeley, CA 94720 USA.

Publisher Item Identifier S 1057-7157(00)01804-7.

I. Introduction

JOULE-HEATING-INDUCED thermal expansion is an important actuation mechanism for microelectromechanical systems (MEMS) [1]–[4]. Many actuation schemes that have been successfully implemented, such as bimetal [5], buckling [6], and thermo-magnetic actuation [7] are based on electro-thermal effects. Empirical characterizations for the performance of these electrothermal actuators, including displacement, force, or functionality are abundant. Analytical solutions, starting from the electrical inputs that provides the joule-heating energy to the mechanical actuation that are the result of thermal-elastic behavior, are often missing. In order to conduct design improvement or optimization for any of these or other electrothermally driven MEMS structures, a clear understanding of electro-thermal-elastic responses is inevitable.

The characterization of electrothermally driven devices consists of two parts: electro-thermal and thermal-elastic analyses. Electrothermal investigation begins with the heating of microstructures by the electrical power. An electro-thermal model for heavily doped polysilicon micro beams was previously established [8]. The model is capable of predicting the temperature distributions on self-heated micromechanical beams. The thermal-elastic problem is investigated in this paper by using the coupled problem of *Elastica* [9]–[11] and the Duhamel-Neumann relation (e.g., [12]). Microstructures fabricated by the MCNC Multi-User MEMS Process (MUMPs) [13] are tested experimentally to verify the analytical model. Moreover, results from a finite-element simulation program are compared with the theoretical derivations and experiments. This coupled electro, thermal, and elastic model has been utilized in the analysis of a vertically driven microactuator [6]. In addition, this model is expected to play an essential role for the development of other MEMS actuators that are based on the electrothermal joule-heating effects such as Heactuators [14] and Hexsil tweezers [15]. In conclusion, the influence of temperature, material and critical design issues are discussed.

1057–7157/00$10.00 © 2000 IEEE

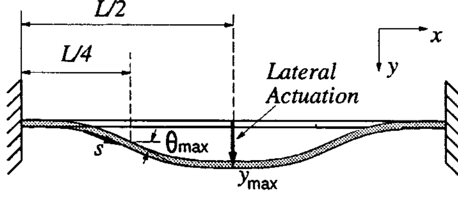

Fig. 1. Clamped–clamped micro beam buckles under joule heating.

II. Theoretical Study

Fig. 1 shows the schematic diagram of a clamped–clamped micro beam that is investigated in this paper. When an electrical current is applied, the outcome of the electro-thermal heating effect causes the beam to expand. The thermal-elastic behavior results in buckling and actuation of the structure. If the width of the structure is less than its thickness, the beam moves laterally, as shown. On the other hand, if the width of the beam is larger than the beam thickness, vertical deflection is expected. The expansion and actuation mechanisms consist of two parts: the electro-thermal response due to the electrical heating and the thermal-elastic reaction due to the thermal expansion of the microstructures.

A. Electro-Thermal Analysis

When an electrical current is applied, resistive heating occurs and the temperature on the beam can be represented as a function of the input current. Previously, an electro-thermal model for suspended microstructures has been investigated with experimental verification [8]. An electrothermal equation was established and the steady-state temperature distribution on the suspended beam was represented as

$$T(x) = T_{\rm com} - (T_{\rm com} - T_\infty)\frac{\cosh\left[\sqrt{\epsilon_{\rm com}}\left(x - \frac{L}{2}\right)\right]}{\cosh\left(\sqrt{\epsilon_{\rm com}}\frac{L}{2}\right)}. \tag{1}$$

The average temperature is calculated by integration

$$T_{\rm avg} = T_{\rm com} - (T_{\rm com} - T_\infty)\frac{\tanh\left(\sqrt{\epsilon_{\rm com}}\frac{L}{2}\right)}{\sqrt{\epsilon_{\rm com}}\frac{L}{2}} \tag{2}$$

where

$$T_{\rm com} = T_\infty + \frac{J^2\rho_\infty}{k_p\epsilon_{\rm com}} \tag{3}$$

$$\epsilon_{\rm com} = \frac{k_n k_{\rm air} F}{k_p h_p(k_{\rm air}h_n + k_n {\rm lift})} - \frac{J^2\rho_\infty\xi_p}{k_p} \tag{4}$$

and T_∞ is the ambient temperature, J is the current density, and ρ_∞ is the resistivity of polysilicon at ambient temperature. The symbols h_p, h_n, and lift represent the thickness of polysilicon, silicon nitride and the suspension gap, respectively. k_n represents the thermal conductivity of silicon nitride. F is the excessive thermal conductive shape factor that can be calculated by using numerical simulations [16]. The thermal resistivity coefficient and the thermal conductivity of polysilicon are represented by ξ_p and k_p. These parameters are experimentally characterized [3], [8], [13], [17], [27] as listed in Table I.

TABLE I
PHYSICAL PROPERTIES OF THE MICRO BEAM

Symbols	Unit	Value	Reference
k_p	$W\ ^\circ C^{-1}\ m^{-1}$	34.0	[8]
α	$^\circ C^{-1}$	2.6 $\times 10^{-6}$	[17], [3]
ξ_p-POLY1	$^\circ C^{-1}$	1.35 $\times 10^{-3}$	[27]
ξ_p-POLY2	$^\circ C^{-1}$	1.14 $\times 10^{-3}$	[27]
ρ_∞-POLY1	$ohm - cm$	0.00184	[13]
ρ_∞-POLY2	$ohm - cm$	0.00247	[13]
F-POLY1-2μm wide	none	4.07	[8]
F-POLY1-1μm wide	none	6.85	[8]
F-POLY2-1μm wide	none	8.06	[8]

B. Thermal-Elastic Analysis

Temperature rise as provided by the electrothermal power causes these beams to elongate. Due to the clamped–clamped boundary condition, compressive stress is generated and buckling behavior occurs if the stress exceeds a critical value. This thermal-elastic problem can be modeled by solving the classical problem of *Elastica* with the governing equation [9], [10]

$$\frac{d^2\theta}{ds^2} + \frac{P}{EI}\sin\theta = 0. \tag{5}$$

As shown in Fig. 1, θ is the deflection angle with respect to the original axial axis, x, and s is the coordinate along the deflected beam. E and I are the Young's modulus and moment of inertia of the beam, respectively. P is the thermal loading and y is the lateral deflection that is solved analytically as [18]

- $0 < x < (L/4)$

$$y = \frac{2\beta}{\sqrt{\frac{P}{EI}}}(1 - \cos\phi) \tag{6}$$

- $(L/4) < x < (L/2)$

$$y = \frac{2\beta}{\sqrt{\frac{P}{EI}}}(1 + \cos\phi) \tag{7}$$

where

$$\beta = \sin\frac{\theta_{\rm max}}{2} \tag{8}$$

$$\phi = \sin^{-1}\left(\frac{\sin\frac{\theta}{2}}{\beta}\right). \tag{9}$$

The maximum deflection angle occurs at one-forth of the beam length due to symmetry and the maximum deflection $y_{\rm max}$ is at the center that can be derived from (7)

$$y_{\rm max} = \frac{4\beta}{\sqrt{\frac{P}{EI}}}. \tag{10}$$

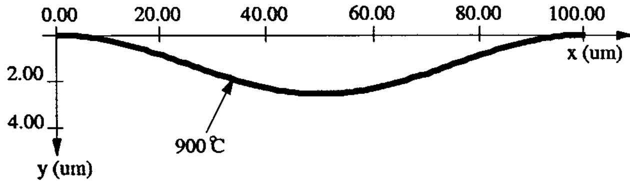

Fig. 2. Simulation result of the deflection shape of a buckled micro beam.

A one-dimensional *Duhamel-Neumann* constitutive law is then used to relate the thermal stress [12] with respect to temperature changes. This step also connects the electro-thermal analysis to the thermal-elastic problem

$$\frac{-P}{A} = E\varepsilon - \alpha E(T - T_\infty) \tag{11}$$

where ε is the thermal strain [18]. A is the cross-sectional area of the beam, and α is the thermal expansion coefficient. The maximum deflection is now derived with respect to the average temperature of the micro beam as

$$y_{\max} = 4\beta\sqrt{\frac{I/A}{\left[\alpha(T_{\rm com} - T_\infty)\left(1-\frac{\tanh\left(\sqrt{\epsilon_{\rm com}}\,\frac{L}{2}\right)}{\sqrt{\epsilon_{\rm com}}\,\frac{L}{2}}\right)-\varepsilon\right]}}. \tag{12}$$

This equation is used to predict the displacement at the center of the beam.

C. Analytical and Numerical Solutions

In order to solve this statically indeterminate problem, maximum deflection angles are first assumed and the corresponding variables such as thermal loading, strain, and maximum deflection are calculated [18]. Before the buckling temperature, the maximum deflection at the center of the beam remains at zero. The simulation program begins its predictions after this minimum temperature is reached. For standard beams of 100-μm long, 2-μm wide, and 2-μm thick, an input current of 3.5 mA is required to generate an average temperature of 531 °C to initiate buckling. It is found that the corresponding thermal loading is 9.2×10^{-4} N. The displacement of the beam keeps increasing as the applied current is increased, but the thermal load decreases. For example, thermal loading drops from the critical value at the buckling point to 99.8% when the average temperature reaches 1000 °C [18]. This is probably due to the stress relaxation process in the post-buckling stage. This trend was previously reported in classic mechanics [19]. The deflection at the center of the beam, on the other hand, increases as the temperature increases and the relation is nonlinearly governed by (12). Fig. 2 is the results of theoretical simulation for the shape of the micro beam in action by solving (6) and (7). The figure shows that when the average temperature of the micro beam is 900 °C, the deflection is about 3 μm.

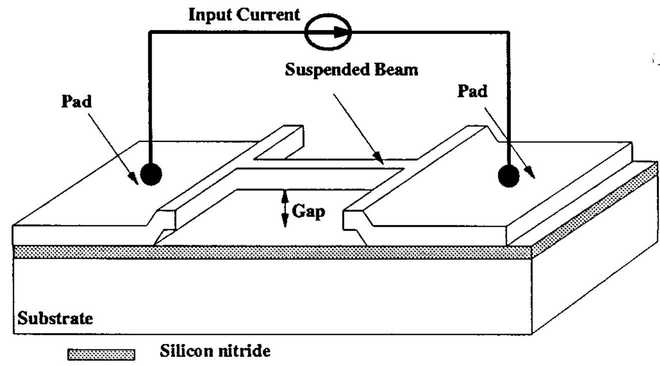

Fig. 3. Schematic diagram of a thermally driven micro beam.

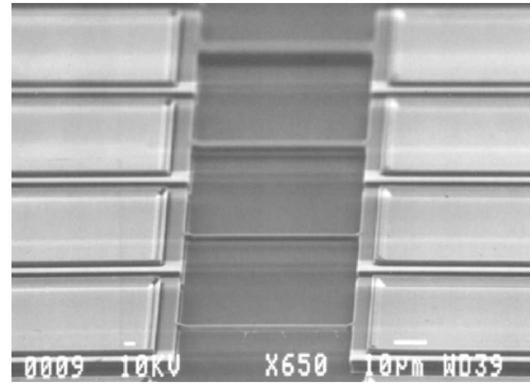

Fig. 4. SEM micrograph of three micro beams with lengths of 50 μm and widths of 1, 2, 5 and 10 μm.

III. Experimental Measurements

A. Sample Preparation and Experimental Setup

The suspended micro beams have been fabricated by the MUMPs in the batch of run #22 [13]. Fig. 3 shows the schematic diagram of the structure. Silicon nitride of 0.6 μm in thickness functions as the thermal and electrical insulation layer. The micro beams are constructed by using the second or third structural layers of heavily phosphorus doped polysilicon in the MUMPs. The POLY1 and POLY2 layers are 2 and 1.5 μm in thickness and suspended 2 and 2.8 μm above the substrate, respectively. Electrical current is supplied via contact pads to the micro beams. Different lengths and widths of micro beams have been designed, fabricated, and tested. The lengths are ranging from 50 to 100 μm with widths of 1, 2, 5, and 10 μm. Fig. 4 is an SEM micrograph showing four suspended micro beams made of POLY1 layer. They are 50-μm long, 10-, 5-, 2-, and 1-μm wide (from top to bottom), respectively. A probe station equipped with a charge-coupled device (CCD) camera and an image-processing card in a personal computer has been utilized in the experiments. The image of the deflected micro beam is captured as shown in Fig. 5. This image is then processed in AutoCAD to measure the lateral deflection, as shown in Fig. 6. The length of micro beam is set as 100-unit length and the corresponding deflection is calculated internally in AutoCAD. In this particular example, the deflection is recorded as 2.9±0.2 μm. The uncertainty of ±0.2 μm is estimated from human errors and the clarity of the image. Both ac and dc inputs have been used to actuate these devices. For ac inputs,

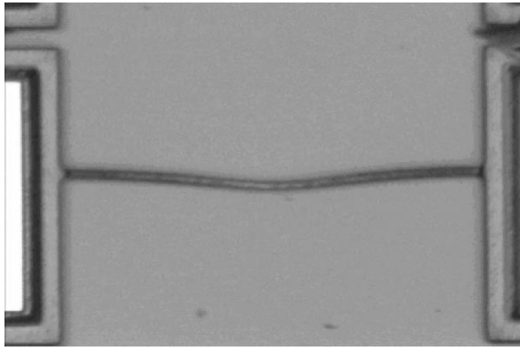

Fig. 5. Image of a micro beam in action under an optical microscope.

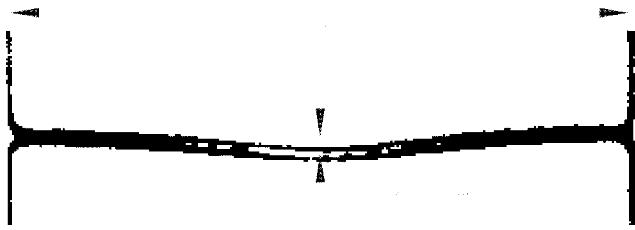

Fig. 6. Deflected image captured and processed in a personal computer by using AutoCAD.

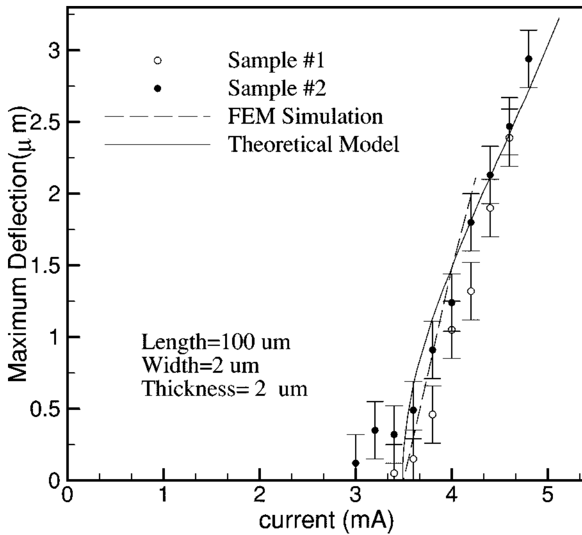

Fig. 7. Plot of the maximum deflection as a function of input current for a $2 \times 2 \times 100\ \mu m^3$ beam.

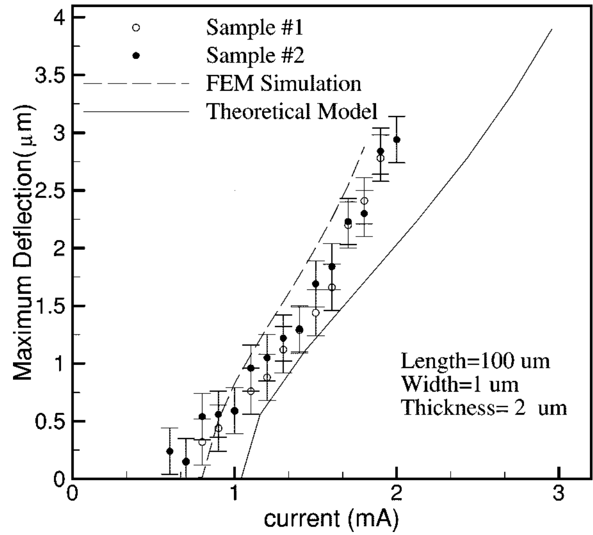

Fig. 8. Plot of the maximum deflection as a function of input current for a $1 \times 2 \times 100\ \mu m^3$ beam.

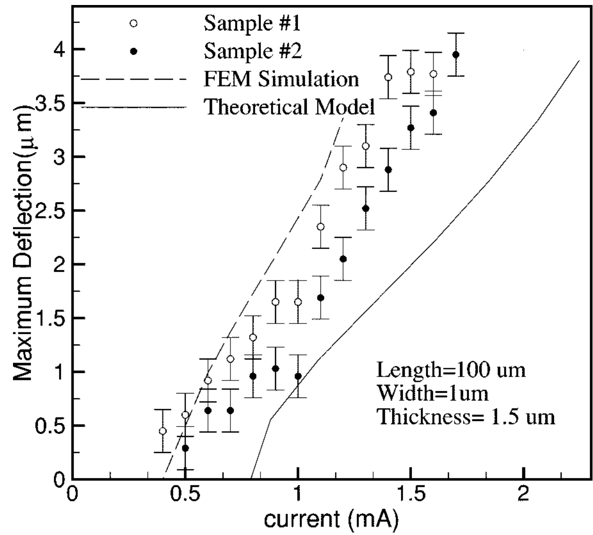

Fig. 9. Plot of the maximum deflection as a function of input current for a $1 \times 1.5 \times 100\ \mu m^3$ beam.

the micro beams move at twice the input frequency up to about 100 Hz. When the input frequency is higher than 100 Hz, the micro beam reacts like it is under dc inputs because the cooling process cannot catch up with the heating process. If the width of the micro beam is less than its thickness, lateral actuation occurs. If its width is larger than the thickness, the micro beam moves vertically.

B. Electrical Input to Mechanical Actuation

Three kinds of micro beams have been tested. They are 100 μm in lengths and 2×2, 1×2 and $1 \times 1.5\ \mu m^2$ in cross sections. Figs. 7–9 show the experimental (symbols) and analytical results. The solid lines are numbers derived from the theoretical model of (12) and the dashed lines are simulations from finite-element analysis (FEA) [20]. In a standard step to analyze this buckling problem, an infinitesimal force is introduced in FEA at the first load step. This infinitesimal force is then removed after bending of the beam. Experimentally, these micro beams do not deflect under low input currents until a critical current is reached to generate a large enough compressive stress for buckling. A simulation result showing temperature versus input current on a $2 \times 2 \times 100\ \mu m^2$ beam is illustrated in Fig. 10. It is calculated that a current of 3.5 mA is required to generate an average temperature of 531 °C to initiate buckling. After buckling, the deflection increases as the input current increases and the experimental measurements are consistent with both the theoretical prediction and FEA simulations. The FEA results seem to be closer to the experiments than the theoretical calculations. The possible explanation is that an average temperature is used in the analytical model while the FEA simulation used the distributed temperature profile that is close to the true conditions. However, FEA simulations require

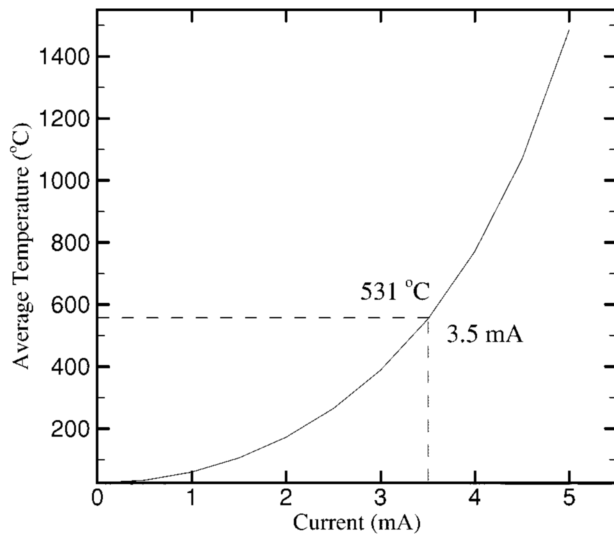

Fig. 10. Average temperature versus input current of heated beam.

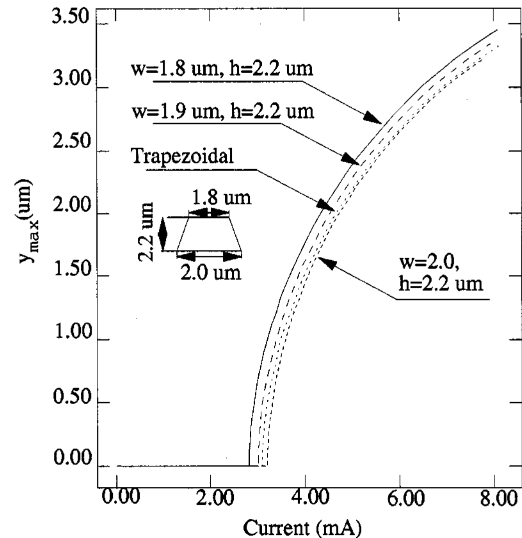

Fig. 11. Effect of geometrical variations.

large computational power for this nonlinear problem. In order to prevent either creep or recrystallization [21], the experiments stop at a temperature of about 900 °C and we found no permanent damages to these devices. For all three kinds of devices, two different samples have been experimentally characterized. In Fig. 7 of the 2×2 μm^2 beams, the experimental results are consistent with the analytical predictions. The analytical predictions underestimate the beam deflections in the cases of 1×2 μm^2 and 1×1.5 μm^2 beams, as shown in Figs. 8 and 9. The major source of discrepancy is that the manufactured widths of these beams are expected to be less than the design widths of 1 μm. Therefore, these beams react at a lower input current as predicted in the theoretical analyses. This over-etching effect also thin those beams of 2 μm in widths in Fig. 7 such that they move laterally instead of vertically. Furthermore, samples with same dimensions do show slightly different experimental results as shown in these figures. This is probably due to the manufacturing variations that cause tiny dimensional variations for the manufactured microstructures.

IV. Discussions

Several modeling considerations are discussed. First, residual stress may exist in micromachined thin films and it is important to characterize its effects. A passive residual strain gauge [22] has been fabricated together with these micro beams via the MCNC MUMPs process, and the residual strains of the POLY2 and POLY3 layers have been detected to be 6.4×10^{-5} compressive. The corresponding residual stresses are 9.6 MPa for polysilicon films with Young's modulus of 150 GPa. When the compressive residual stress is considered in the analysis, the critical current to cause the buckling of micro beams decreases. In fact, self-buckling may occur when there is a great amount of compressive stress is in the thin film, as discussed previously [23], [24]. On the other hand, if the residual stress is tensile, it hinders the actuation of the micro beams. In general, the current-deflection curves as those of Figs. 7–9, move from left to right as the residual stress changes from compressive to tensile.

Process variations may also change the behavior of micro beams. For example, a trapezoidal, instead of a square shape may be the true cross section of the beams as the result of an imperfect reactive-ion-etching process [25]. In addition, the width and thickness of the beams may also vary from different wafers or even different locations of the same wafer. Fig. 11 shows simulation results that characterize the sensitivity of the micro beams with respect to these process variations. The standard beam is 2×2.2 μm^2 in cross section. When the width decreases, the analytical prediction shows that the current-deflection curve moves to the left because the rigidity of the micro beam is reduced. For beams with trapezoidal cross section of 1.8 μm at the top and 2.0 μm at the bottom, the simulation result shows the curve move to the left–hand side, but is very close to the standard beam. In summary, all of these process variations affect the performance of the micro beam and the variations are within 10% of the original current-deflection curve. The variations in material properties with respect to temperature have not been considered in these theoretical models, but in reality, these values change at different temperature [26]. Unfortunately, the databases for material properties with respect to temperature of many thin films, including polysilicon, have not been fully established. A detail study for several "mechanical" properties, including thermal expansion coefficient, thermal conductivity, and Young's modulus is essential to improve the accuracy of this and other MEMS models.

V. Conclusions

A MEMS model that combines both electro-thermal and thermal-elastic analyses has been developed for buckling behavior of micromachined beams. This model can be applied to microstructures that operates based on the principle of joule-heating effects. The transformation of energy is successfully established, from electrical inputs to thermal heating, and to the mechanical deflections. A standard surface micromachining process that was conducted via the foundry service of

MCNC MUMPs is used to fabricate these micro beams. It is found that the experimental measurements are consistent with analytical predictions. The theoretical analysis underestimate the lateral deflections for beams of 1 μm in width probably due to the plasma-etching process that generally thins down the designed width. A typical micro beam with 2 μm in width, 2 μm in thickness, and 100 μm in length can achieve a lateral displacement of 2.9 μm at the center of the beam under a 4.8-mA input current.

ACKNOWLEDGMENT

The authors would like to thank Prof. W. Fang, National Tsing Hua University, Hsin-Chu, Taiwan, R.O.C., for valuable discussions on the post-buckling analysis, Prof. R. A. Scott, The University of Michigan at Ann Arbor, in advising the finite-element analysis, and Y. T. Cheng, The University of Michigan at Ann Arbor, for helping with the SEM work.

REFERENCES

[1] W. Riethmuller and W. Benecke, "Thermally excited silicon microactuators," *IEEE Trans. Electron Devices*, vol. 35, pp. 758–762, June 1988.

[2] B. Hälg, "On a nonvolatile memory cell based on micro-electro-mechanics," in *Proc. IEEE MEMS Workshop*, Feb. 1990, pp. 172–176.

[3] H. Matoba, T. Ishikawa, C. J. Kim, and R. S. Muller, "A bistable snapping microactuator," in *Proc. IEEE MEMS Workshop*, Jan. 1994, pp. 45–50.

[4] J. H. Comtois and V. M. Bright, "Surface micromachined polysilicon thermal actuator arrays and applications," *Solid-State Sens. Actuator Workshop Tech. Dig.*, pp. 174–177, 1996.

[5] S. Timoshenko, "Analysis of bi-metal thermostats," *J. Opt. Soc. Amer.* , vol. 11, p. 233, 1925.

[6] L. Lin and S. H. Lin, "Vertically driven microactuators by electrothermal buckling effects," *Sens. Actuators*, vol. A71, pp. 35–39, 1998.

[7] H. Guckel, J. Klein, T. Christenson, K. Skrobis, M. Laudon, and E. Lovell, "Thermomagnetic metal flexure actuators," *Solid-State Sens. Actuator Workshop Tech. Dig.*, pp. 73–75, 1992.

[8] L. Lin and M. Chiao, "Electrothermal responses of lineshape microstructures," *Sens. Actuators*, vol. A55, pp. 35–41, 1996.

[9] S. P. Timoshenko and J. N. Goodier, *Theory of Elasticity*, 3rd ed. New York: McGraw-Hill, 1970.

[10] C. T. Wang, *Applied Elasticity*. New York: McGraw-Hill, 1953.

[11] M. R. Horne, *The Stability of Frames*. New York: Pergamon, 1965.

[12] Y. C. Fung, *Foundations of Solid Mechanics*. Engelwood Cliffs, NJ: Prentice-Hall, 1965.

[13] K. W. Markus and D. S. Koester, "Multi-user MEMS process (MUMPs) introduction and design rules," MCNC Electron., Oct. 1994.

[14] R. P. Reid, V. M. Bright, and J. H. Comtois, "Force measurements of polysilicon thermal microactuators," *SPIE Micromach. Devices Comp. II*, vol. 2882, pp. 296–306, 1996.

[15] C. G. Keller and R. T. Howe, "Hexsil tweezers for teleoperated microassembly," in *Proc. IEEE MEMS Workshop*, 1997, pp. 72–77.

[16] L. Lin, "Selective encapsulations of MEMS: Micro channels, needles, resonators and electromechanical filters," Ph.D. dissertation, ME Dept. Univ. California at Berkeley, Berkeley, CA, 1993.

[17] T. Lisec, S. Hoerschelmann, H. J. Quenzer, B. Wanger, and W. Benecke, "Thermally driven microvalve with buckling behavior for pneumatic applications," in *Proc. IEEE MEMS Workshop*, Jan. 1994, pp. 13–17.

[18] L. Lin and M. Chiao, "Electro, thermal and elastic characterization of suspended micro beams," *Microelectron. J.*, vol. 29, no. 4–5, pp. 269–276, 1998.

[19] O. Mahrenholtz, G. Ioannidis, and A. N. Kounadis, "Lateral post-buckling analysis of beams," *Archive Appl. Mechan.*, vol. 63, pp. 151–158, 1993.

[20] ANSYS, *Finite Element Analysis Program*. Houston, TX: Swanson Anal. Syst. Inc., 1990.

[21] T. Akiyama, Y. Fukuta, and H. Fujita, "A reshaping technology with joule heat for three dimensional silicon structures," in *Dig. 8th. Solid-State Sens. Actuators, Transducers '95 Int. Conf*, pp. 174–177.

[22] L. Lin, A. P. Pisano, and R. T. Howe, "A micro strain gauge with mechanical amplifier," *IEEE J. Microelectromech. Syst.*, vol. 6, pp. 313–321, Dec. 1997.

[23] H. Guckel, T. Randazzo, and D. W. Burns, "A simple technique for the determination of mechanical strain in thin films with applications to polysilicon," *J. Appl. Phys.*, vol. 57, pp. 1671–1675, 1985.

[24] W. Fang and J. A. Wickert, "Post-buckling of micromachined beams," in *Proc. IEEE MEMS Workshop*, Jan. 1994, pp. 182–187.

[25] W. C. Tang, M. G. Lim, and R. T. Howe, "Electrostatic comb drive levitation and control method," *IEEE J. Microelectromech. Syst.*, vol. 1, pp. 170–178, Dec. 1992.

[26] C. W. Bert and C. Fu, "Implications of stress dependency of the thermal expansion coefficient on thermal buckling," *ASME J. Pressure Vessel Technol.*, vol. 114, pp. 189–192, May 1992.

[27] Y. T. Cheng, L. Lin, and K. Najafi, "Localized silicon fusion and eutetic bonding for MEMS fabrication and packaging," *Solid-State Sens. Actuator Workshop*, pp. 233–236, June 1998.

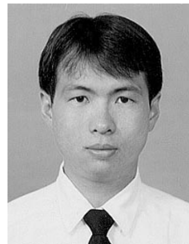

Mu Chiao received the B.S. degree in agricultural machinery engineering and M.S. degree in applied mechanics from the National Taiwan University, Taiwan, R.O.C., in 1994 and 1996, respectively, and is currently working toward the Ph.D. degree in MEMS design, fabrication and packaging at the University of California at Berkeley.

Liwei Lin (S'92–M'93) received the B.S. degree in power mechanical engineering from the National Tsing Hua University, Taiwan, R.O.C., in 1986, and the M.S. and Ph.D. degrees in mechanical engineering from the University of California at Berkeley, in 1991 and 1993, respectively.

From 1993 to 1994, he was with BEI Electronics Inc., where he was involved in research and development of microsensors. From 1994 to 1996, he was an Associate Professor at the Institute of Applied Mechanics, National Taiwan University, Taiwan, R.O.C. From 1996 to 1999, he was an Assistant Professor in the Mechanical Engineering and Applied Mechanics Department, The University of Michigan at Ann Arbor. Since 1996, he has been an Assistant Professor in the Mechanical Engineering Department and Associate Director in Berkeley Sensor and Actuator Center, University of California at Berkeley. His research interests are in MEMS, including design, modeling and fabrication of microstructures, microsensors, and microactuators packaging. He holds six U.S. patents in the area of MEMS.

Dr. Lin led the effort in establishing the MEMS Subdivision of the American Society of Mechanical Engineers (ASME) and is currently serving as the vice chairman of the Executive Committee for the MEMS Subdivision.